

LA-UR-21-20765

Accepted Manuscript

Bohm Criterion of Plasma Sheaths away from Asymptotic Limits

Li, Yuzhi
Srinivasan, Bhuvana
Tang, Xianzhu

Provided by the author(s) and the Los Alamos National Laboratory (2022-06-22).

To be published in: Physical Review Letters

DOI to publisher's version: 10.1103/PhysRevLett.128.085002

Permalink to record:

<http://permalink.lanl.gov/object/view?what=info:lanl-repo/lareport/LA-UR-21-20765>



Los Alamos National Laboratory, an affirmative action/equal opportunity employer, is operated by Triad National Security, LLC for the National Nuclear Security Administration of U.S. Department of Energy under contract 89233218CNA000001. By approving this article, the publisher recognizes that the U.S. Government retains nonexclusive, royalty-free license to publish or reproduce the published form of this contribution, or to allow others to do so, for U.S. Government purposes. Los Alamos National Laboratory requests that the publisher identify this article as work performed under the auspices of the U.S. Department of Energy. Los Alamos National Laboratory strongly supports academic freedom and a researcher's right to publish; as an institution, however, the Laboratory does not endorse the viewpoint of a publication or guarantee its technical correctness.

Bohm criterion of plasma sheaths away from asymptotic limits

Yuzhi Li,¹ Bhuvana Srinivasan,¹ Yanzeng Zhang,² and Xian-Zhu Tang²

¹Kevin T. Crofton Department of Aerospace and Ocean Engineering, Virginia Tech, Blacksburg, Virginia 24060

²Theoretical Division, Los Alamos National Laboratory, Los Alamos, New Mexico 87545

(Dated: 28 January 2022)

The plasma exit flow speed at the sheath entrance is constrained by the Bohm criterion. The so-called Bohm speed regulates the plasma particle and power exhaust fluxes to the wall, and it is commonly deployed as a boundary condition to exclude the sheath region in quasi-neutral plasma modeling. Here the Bohm criterion analysis is performed in the intermediate plasma regime away from the previously known limiting cases of adiabatic laws and the asymptotic limit of infinitesimal Debye length in a finite-size system, using the transport equations of an anisotropic plasma. The resulting Bohm speed has explicit dependence on local plasma heat flux, temperature isotropization, and thermal force. Comparison with kinetic simulations demonstrates its accuracy over the plasma-sheath transition region in which quasineutrality is weakly perturbed and Bohm criterion applies.

Sheath theory has a central place in plasma physics as its original formulation coincided with the recognition of plasma physics as a sub-field in physics^{1,2} and it applies to any plasma bounded by a material boundary³⁻⁷. One of the most celebrated findings in sheath theory is the so-called Bohm criterion⁸⁻¹⁴ that predicts a threshold, the so-called Bohm speed, which would provide a lower bound for the plasma exit flow speed at the sheath entrance. Bohm criterion (also known as sheath criterion in the literature) is an inequality at the sheath entrance, which can be written as⁹

$$\left(\frac{\partial n_e}{\partial \phi} - Z \frac{\partial n_i}{\partial \phi} \right) \Big|_{\phi=\phi^{se}} \geq 0. \quad (1)$$

Here $n_{e,i}$ denote the electron and ion density, respectively, ϕ is the plasma potential, and the superscript se labels the sheath entrance where the plasma transitions from quasi-neutral in the presheath to non-neutral inside the sheath. A straightforward^{8,9}, but not necessarily unique^{10,11}, physics interpretation of Bohm criterion is that Eq. (1) is required for the plasma potential to have non-oscillatory solutions into the sheath. This can be understood by linearizing the Poisson equation for ϕ in the neighborhood of the sheath entrance where $n_e \approx Zn_i$ remains a good approximation. The solution is of an exponential form with the exponent imaginary if Eq. (1) is violated, indicating an oscillatory ϕ into the sheath, which would contradict the expectation of monotonically varying ϕ that slows down the electrons for ambipolarity⁹.

Traditionally, evaluation of Bohm speed from the Bohm criterion invokes drastic simplification of plasma transport. These are normally expressed in terms of varying γ in the adiabatic law $pn^{-\gamma} = \text{constant}$. For example, $\gamma = 1$ for an isothermal plasma, $\gamma = 5/3$ for an ideal plasma having three degrees of freedom, and $\gamma = 3$ for an ideal plasma constrained to one degree of freedom. The Bohm speed in these limiting cases then equals the sound speed¹¹

$$u_{Bohm} = c_s(\gamma_e, \gamma_i) \equiv \sqrt{(\gamma_e T_e^{se} + \gamma_i T_i^{se}) / m_i}. \quad (2)$$

It is interesting to note that although Bohm⁸ originally invoked the isothermal electron approximation to realize the $\gamma_e = 1$ case of Eq. (2), subsequent work¹⁵ had relaxed the requirement to a Boltzmann distribution for the electron density,

$n_e = n_0 \exp(e\phi/T_e^*)$, with ϕ the plasma potential and T_e^* an effective or screening temperature, the latter of which is interpreted as what Langmuir probes are supposed to measure.

It was recognized early on⁹ that transport in the neighborhood of the sheath can greatly complicate the physics constraint set by the Bohm criterion. A large body of work^{10,11,16-18} has since been devoted to the development of the so-called kinetic Bohm criterion, which is obtained by integrating the kinetic equation for $n_{i,e}$ in Eq. (1). The standard expression bears the form

$$\frac{1}{m_i} \int d^3\mathbf{v} \frac{f_i(\mathbf{v})}{v_z^2} \leq -\frac{1}{m_e} \int d^3\mathbf{v} \frac{1}{v_z} \frac{\partial f_e(\mathbf{v})}{\partial v_z} \quad (3)$$

with $m_i(m_e)$ the ion (electron) mass, $f_i(f_e)$ the ion (electron) distribution function, and velocity v_z which is normal to the wall in an unmagnetized plasma or parallel to the magnetic field in a magnetized plasma. A recent debate^{12,19,20} highlighted a profound disconnect between (1) the conventional theory of the Bohm criterion and (2) the practical needs in plasmas that we normally encounter. Specifically, the Bohm criterion like in Eq. (3) was derived in the asymptotic limit of $\lambda_D/L \rightarrow 0$ ¹⁹ with λ_D the Debye length and L the plasma size, while plasmas of practical interest are frequently away from this asymptotic limit²⁰. The underlying challenge echoes back to an earlier discussion²¹⁻²⁶ on where the sheath entrance or edge resides, an intimately connected issue since that is where the Bohm criterion is supposed to be applied.

The complication is that between the quasineutral plasma and the non-neutral Debye sheath in a plasma away from the asymptotic limit of $\lambda_D/L \rightarrow 0$, there is usually a transition layer in which the quasineutrality is weakly violated, and the plasma flow and potential (and its gradient and hence electric field) can vary gradually²⁵⁻²⁸. Matched asymptotic analysis of a simplified plasma model with isothermal electrons and cold ions, reveals that the plasma ion flow actually crosses the classically defined Bohm speed⁸ $u_{Bohm} = \sqrt{T_e/m_i}$ somewhere inside this transition layer^{26,27}. This is consistent with the straightforward interpretation of the Bohm criterion as given in Eq. (1) by Harrison and Thompson⁹ that (1) it offers no meaningful constraint in the quasineutral region because $n_e \approx Zn_i$ and Poisson's equation is not used for evaluating ϕ ;

(2) it does not apply in the Debye sheath in the sense of Langmuir and Tonks^{1,2} since n_e grossly differs from Zn_i , and (3) it does impose a constraint, as we shall show in this Letter, on the ion flow speed over the *spatially extended transition region*, as opposed to a *sharp transition boundary*, over which quasineutrality is mildly perturbed so charge density gradient is the dominant term upon linearization of Poisson's equation. This last point implies a Bohm speed that should *vary inside this transition region*.

In this Letter, we derive an expression for the Bohm speed away from the previously known asymptotic limits, that elucidates the distinct roles of various transport physics, including heat flux, collisional isotropization, and thermal force for both electron and ion transport. Its explicit dependence on plasma transport and local electric field suggests a spatially varying Bohm speed over a transition region in which quasineutrality is weakly perturbed. This is confirmed by first-principle kinetic simulations over a range of plasma collisionality. To our knowledge, this is the first time that *a predictive formula for Bohm speed has been shown to be quantitatively accurate in the intermediate plasma regime that is away from the limiting cases of adiabatic laws and the asymptotic limit of $\lambda_D/L \rightarrow 0$.*

The nature of plasma transport in the sheath/presheath region is governed by the sheath Knudsen number K_n , which is the ratio between plasma mean-free-path λ_{mfp} and the Debye length λ_D . In cases of most interest, $K_n > 1$ or $K_n \gg 1$. A consequence is that within the Knudsen layer, which is defined as one mean-free-path (λ_{mfp}) within the wall, streaming loss and the associated decompressional cooling would induce robust temperature anisotropy²⁹, $T_{\parallel} < T_{\perp}$. The parallel degree of freedom is along the magnetic field, or in an unmagnetized plasma the plasma flow direction, which is normal to the wall surface. Due to the anisotropic nature of the plasma, the mean-free-path is defined as $\lambda_{mfp} \equiv v_{the}/\nu_{ei}$ with $v_{the} = \sqrt{T_{e\parallel}/m_i}$ the electron thermal velocity and ν_{ei} the electron-ion collision frequency in an anisotropic plasma given by Eq. (7). Here we will focus on a magnetized plasma, with a uniform magnetic field normal to the wall ($T_{\parallel} = T_x$) and y signifying a perpendicular direction ($T_{\perp} = T_y$). The plasma transport equations that directly enter the Bohm speed evaluation include the species continuity equation, momentum equation, and energy equation, all in the parallel or x direction, which in the neighborhood of the sheath entrance, take the form,

$$\frac{\partial n_e u_{ex}}{\partial x} = 0; \quad \frac{\partial n_i u_{ix}}{\partial x} = 0, \quad (4a)$$

$$\frac{\partial n_e T_{ex}}{\partial x} = en_e \frac{\partial \phi}{\partial x} - \alpha n_e \frac{dT_{ex}}{dx}, \quad (4b)$$

$$n_i m_i u_{ix} \frac{\partial u_{ix}}{\partial x} + \frac{\partial n_i T_{ix}}{\partial x} = -Zen_i \frac{\partial \phi}{\partial x} + \alpha n_e \frac{dT_{ex}}{dx}, \quad (4c)$$

$$n_e u_{ex} \frac{\partial T_{ex}}{\partial x} + 2n_e T_{ex} \frac{\partial u_{ex}}{\partial x} + \frac{\partial q_n^e}{\partial x} = Q_{ee} + Q_{ei}, \quad (4d)$$

$$n_i u_{ix} \frac{\partial T_{ix}}{\partial x} + 2n_i T_{ix} \frac{\partial u_{ix}}{\partial x} + \frac{\partial q_n^i}{\partial x} = Q_{ii}. \quad (4e)$$

Here we have ignored the electron inertia and a net plasma current into the wall, α is the thermal force coefficient, $q_n^{e,i}$ are the heat flux of x -degree of freedom in the x direction,

$$q_n \equiv \int m (v_x - u_x)^3 f d^3 \mathbf{v}, \quad (5)$$

and (Q_{ee}, Q_{ei}, Q_{ii}) are temperature isotropization terms in an anisotropic plasma, which in high collisionality limit³⁰ have the form,

$$Q_{ee} \approx \frac{\sqrt{2}}{2} Q_{ei} = 8n_e v_{ee} T_{ey} \frac{T_{ex}}{T_{ey} - T_{ex}} \left[-3 + \left(3 \sqrt{\frac{T_{ex}}{T_{ey} - T_{ex}}} + \sqrt{\frac{T_{ey} - T_{ex}}{T_{ex}}} \right) \arctan \sqrt{\frac{T_{ey} - T_{ex}}{T_{ex}}} \right], \quad (6)$$

with the collision rate

$$v_{ee} = \frac{n_e v_{ei}}{n_i \sqrt{2}} = \frac{\sqrt{\pi}}{2} n_e \frac{e^4}{(4\pi\epsilon_0)^2} \frac{\ln \Lambda}{\sqrt{m_e T_{ex} T_{ey}}}. \quad (7)$$

The evaluation of the Bohm speed can now be performed following Ref.³¹. Combining the electron continuity equation, momentum equation, and energy equation, we can substitute out the $\partial T_{ex}/\partial x$ and $\partial u_{ex}/\partial x$ terms and find that in the neighborhood of the sheath entrance where ϕ is a monotonically varying function of x ,

$$\frac{\partial n_e}{\partial \phi} = \frac{en_e}{(3+2\alpha)T_{ex}} + \frac{1+\alpha}{(3+2\alpha)u_{ex}T_{ex}} \left(\frac{\partial q_n^e}{\partial \phi} + \frac{Q_{ee} + Q_{ei}}{E} \right) \quad (8)$$

where $E = -\partial \phi / \partial x$ is the electric field. In contrast, the ion inertia must be retained in a similar analysis of the ion continuity, momentum, and energy equations, and the result is

$$\frac{\partial n_i}{\partial \phi} = \frac{1}{3u_{ix}T_{ix} - m_i u_{ix}^3} \left(\frac{\partial q_n^i}{\partial \phi} + \frac{Q_{ii}}{E} \right) - \frac{Zen_i - \alpha n_e \partial T_{ex} / \partial \phi}{3T_{ix} - m_i u_{ix}^2}. \quad (9)$$

Substituting Eqs. (8) and (9) into Eq. (1), and rearranging terms, we find that the Bohm criterion provides a lower bound for the plasma exit flow speed,

$$u_{ix}^{se} \geq u_{Bohm} \quad (10)$$

with

$$u_{Bohm} \equiv \sqrt{\frac{Z\beta T_{ex}^{se} + 3T_{ix}^{se}}{m_i}}, \quad (11)$$

and

$$\beta \equiv \frac{3 - \frac{3+2\alpha}{Ze\Gamma_i^{se}} \left(\frac{\partial q_n^i}{\partial \phi} + \frac{Q_{ii}}{E} \right) + \frac{\alpha}{e\Gamma_e^{se}} \left(\frac{\partial q_n^e}{\partial \phi} + \frac{Q_{ee} + Q_{ei}}{E} \right)}{1 + \frac{1+\alpha}{e\Gamma_e^{se}} \left(\frac{\partial q_n^e}{\partial \phi} + \frac{Q_{ee} + Q_{ei}}{E} \right)}. \quad (12)$$

Here $\Gamma_{e,i} = n_{e,i} u_{ex,ix}$, and all quantities on the right hand side of Eq.(12) are evaluated locally at the sheath entrance, which is interpreted here as the plasma-to-sheath transition region where quasineutrality is weakly violated.

The Bohm speed defined in Eqs. (11,12) takes into account the known collisional transport physics. It recovers the collisionless sheath/presheath limit previously found in Ref.³¹, which is obtained by setting α , Q_{ee} , Q_{ei} , and Q_{ii} to zero,

$$\beta = \left(3 - \frac{3}{Ze\Gamma_e^{se}} \frac{\partial q_n^i}{\partial \phi} \right) / \left(1 + \frac{1}{e\Gamma_e^{se}} \frac{\partial q_n^e}{\partial \phi} \right) \quad (13)$$

A particularly interesting limit is $L \gg \lambda_{mfp} \gg \lambda_D$ so the upstream plasma is a Maxwellian. The presheath/sheath electrons follow a truncated bi-Maxwellian due to the trapping effect of the ambipolar electrostatic potential, which gives rise to an electron heat flux that satisfies $\partial q_n^e / \partial \phi = 2e\Gamma_e^{se}$.³² Ignoring the much smaller ion heat flux, one then finds $u_{Bohm} = \sqrt{(T_{ex} + 3T_{ix})/m_i}$ because of the dominant contribution from the electron heat flux term.³¹ This strikes a remarkable but superficial coincidence with the Bohm speed expression in Eq. (2) for $c_s(\gamma_e = 1, \gamma_i = 3)$.

The full expression in Eq. (12) allows us to quantify the transport physics effect on Bohm speed over a wide range of plasma collisionality. Perhaps the subtlest factor is the collisional temperature isotropization. Naively, one would expect Q_{ee} to be small when plasma collisionality is either strong in which case $T_y - T_x$ vanishes, or weak in which case v_{ee} becomes negligibly small. This can be quantitatively assessed by expanding Q_{ee} in the small parameter of $X \equiv \sqrt{(T_{ey} - T_{ex})/T_{ex}}$. To leading order in X , the collisional closure of Chodura and Pohl³⁰ predicts

$$Q_{ee} = \frac{32}{15} n_e v_{ee} T_{ey} X^2. \quad (14)$$

The collisional temperature isotropization enters the Bohm speed with normalization by the electron flux and electric field at the sheath entrance,

$$\begin{aligned} \frac{Q_{ee} + Q_{ei}}{e\Gamma_e E} &\approx (1 + \sqrt{2}) \frac{32}{15} \frac{n_e v_{ee} T_{ey} X^2}{e n_e u_{ex} E} \\ &= (1 + \sqrt{2}) \frac{32}{15} \frac{v_{th,e}}{u_{ex}^{se}} \frac{\lambda_D}{\lambda_{mfp}} \frac{T_{ey}}{eE\lambda_D} X^2 \\ &\approx (1 + \sqrt{2}) \frac{32}{15} \sqrt{\frac{T_{ex}^{se}}{\beta T_{ex}^{se} + 3T_{ix}^{se}}} \frac{\sqrt{m_i/m_e}}{K_n} \frac{T_{ey}}{\lambda_D e E} X^2. \end{aligned} \quad (15)$$

In the collisionless sheath limit $K_n \rightarrow \infty$ but all the other terms are bounded so

$$\lim_{K_n \rightarrow \infty} \frac{Q_{ee} + Q_{ei}}{e\Gamma_e E} = 0, \quad (16)$$

which is the limiting result to be expected. In the intermediate regime of finite collisionality, different offsetting physics can produce an order-unity $(Q_{ee} + Q_{ei})/e\Gamma_e E$ that has an indispensable role in setting the Bohm speed. In the high collisionality regime, which is denoted by $K_n < \sqrt{m_i/m_e}$, the small but

still finite temperature anisotropy is the offsetting factor that produces a $(Q_{ee} + Q_{ei})/e\Gamma_e E \sim O(1)$. With a decreasing collisionality so $K_n > \sqrt{m_i/m_e}$ but not too much greater, there are two offsetting factors coming into play. The first is the familiar temperature anisotropy, which can be enhanced by an order of magnitude. The second is a much reduced electric field at the sheath entrance, which can boost the factor $T_{ey}/\lambda_D e E$. Overall, one finds that for a range in which $K_n > \sqrt{m_i/m_e}$, the two effects can offset a large K_n , so $(Q_{ee} + Q_{ei})/e\Gamma_e E$ remains order unity and hence has an important role in setting the Bohm speed.

Next we deploy first-principle kinetic simulations to verify the Bohm speed of Eq. (11,12) and quantify the relative importance of various transport physics under consideration. The VPIC³³ simulations are for a slab plasma bounded by absorbing walls at $x = 0$ and $x = L$. The loss at the wall is balanced by a plasma source in the middle $x \in [3/8L, 5/8L]$, as a way to mimic the upstream source for the scrape-off layer plasma in a tokamak. Other specifics include $L = 256\lambda_D$, $N = 10000$ markers per cell, $Z = 1$, $m_i/m_e = 1836$. The source temperatures $T_{e0} = T_{i0}$ and the background or initial plasma density n_0 will be varied so the sheath Knudsen number $K_n \in [20, 5000]$. The uniform magnetic field is strong so the plasma beta is much less than unity, $\sim 1\%$. At the sheath entrance K_n^e would be smaller, but proportional to K_n . There are three essential points we will focus on here.³⁴

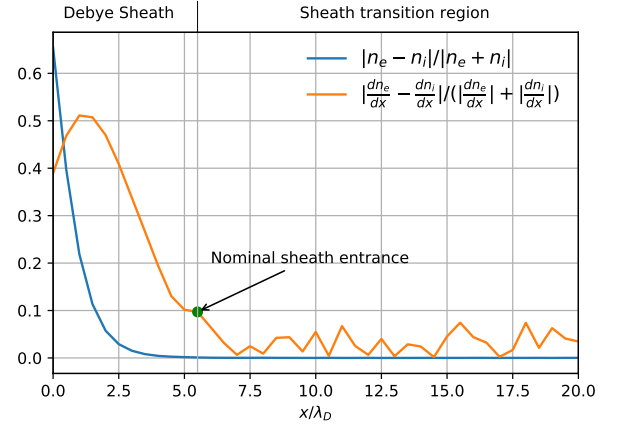


FIG. 1: The normalized net charge density $\bar{\rho}$, and the fractional charge density gradient $\partial \rho / \partial x$ for $K_n = 200$.

The first point is on the sheath entrance, which for a plasma away from the asymptotic limit of $\lambda_D/L \rightarrow 0$, covers a transition region in which deviation from quasineutrality is small but finite. The transition into the sheath can be most obviously assessed by fractional charge density $|n_e - n_i|/(n_e + n_i)$, but a more sensitive measure for Bohm criterion is $|\partial n_e / \partial x - \partial n_i / \partial x| / (|\partial n_e / \partial x| + |\partial n_i / \partial x|)$. In Fig. 1, one can see that with the PIC noise of $N = 10000$ markers per cell, we can reliably position the edge of the sheath transition region to $x > 5\lambda_D$ using the charge density gradient, while the charge density itself gives a sensitivity to $x = 2.5\lambda_D$. The simulation data of the fractional charge density gradient, which has

higher sensitivity, is consistent with a sheath transition region over which the violation of quasineutrality is small, and proceeds gradually towards the non-neutral Debye sheath.

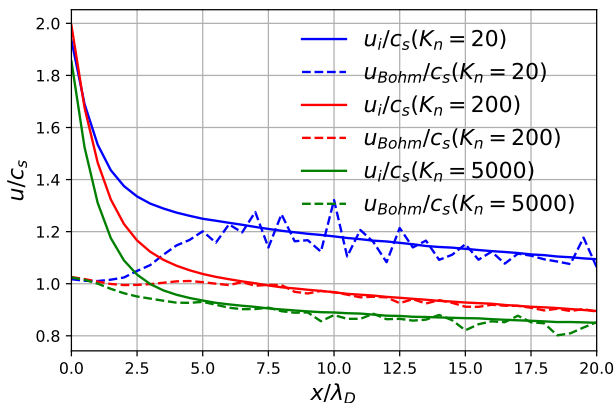


FIG. 2: Ion exit flow speed from simulation data and Bohm speed calculated from Eq. (11,12) normalized by $c_s(\gamma_e = 1, \gamma_i = 3)$ in Eq. (2) over distance from wall for $K_n = 20, 200, 5000$. The breakdown of u_{Bohm} from Eq. (11,12) for Bohm speed is an accurate indication of transitioning into non-neutral Debye sheath.

The second point is that over the *spatially extended sheath transition region*, the Bohm criterion should be applicable with a high degree of accuracy that is measured by the fractional change in charge density gradient. In Fig. 2, we contrast the ion flow speed from VPIC simulations, with the Bohm speed from Eq. (11,12), as a function of position from the wall. Here, in evaluating the Bohm speed, we compute all individual terms in Eq. (12) using the VPIC simulation data. Since the terms in Eq. (12) involve higher-order velocity moments and their derivatives, we deploy time-averaging (but not spatio-averaging) over a long period in which the plasma has reached steady-state. This overcomes the constraint of the normal PIC noise level of $1/\sqrt{N}$ with N the particle markers per cell. The inherent PIC noise has been sufficiently suppressed that we can see a clear sheath transition region over which the ion flow speed closely follows the Bohm speed of Eq. (11,12) in Fig. 2. Further into the Debye sheath, the ion flow speed diverges from the locally evaluated Bohm speed to become significantly greater, as expected. Further away from the Debye sheath and wall, the theoretical expectation is that Eq. (11,12) would set a local Bohm speed as long as it is still within the transition region where quasineutrality is weakly perturbed. It must be emphasized that in the quasineutral region, the Bohm criterion as of Eq. (1) is not a viable concept, so Eq. (1) no longer produces a physically meaningful speed to constrain the ion flow.

The third point is on the relative importance of various transport physics in setting the Bohm speed. The transport under examination is collisional by nature, and includes thermal force, heat flux, and collisional temperature isotropization, for both electrons and ions. We are particularly interested in how these dependencies vary (a) with collisionality

TABLE I: Sheath quantities (columns) around the nominal sheath entrance (x/λ_D) for nominal³⁶ $K_n = (20, 200, 5000)$ cases (rows), with K_n^{se} the local Knudsen number.

K_n^{se}	x/λ_D	u_{ix}/c_s	u_{Bohm}/c_s	$\frac{1}{e\Gamma_e^{se}} \frac{\partial q_n^e}{\partial \phi}$	$\frac{Q_{ee}^{se} + Q_{ei}^{se}}{e\Gamma_e^{se} E^{se}}$	$\frac{1}{e\Gamma_i^{se}} \frac{\partial q_n^i}{\partial \phi}$	$\frac{Q_{ii}^{se}}{e\Gamma_i^{se} E^{se}}$	α^{se}
5.26	5.0	1.25	1.20	-1.63	1.48	-0.05	0.18	0.59
50.0	5.5	1.02	1.00	-2.20	3.55	-0.22	0.38	0.45
1932	5.0	0.94	0.93	0.23	1.17	0.52	0.07	0.04

K_n and (b) over space in the transition layer of a given K_n . For (a), we contrast the ion flow speed with the Bohm speed at a nominal sheath entrance point for different nominal K_n cases. The terms in Eq. (12) are computed from simulation data and separately tabulated in Table I to quantify their relative importance³⁷. Also shown are the local sheath Knudsen number K_n^{se} , ion exit flow speed u_{ix} directly from simulations, and u_{Bohm} computed from Eq. (11,12) using the tabulated data for each case. Both u_{ix} and u_{Bohm} are normalized by $c_s(\gamma_e = 1, \gamma_i = 3)$ from Eq. (2), using T_{ex}^{se} and T_{ix}^{se} from the simulations. The electron thermal flux enters through a divergence in the energy equation, so it is a dominant term in sheath analysis³¹. This is clearly indicated by the data, with additional subtleties in the high K_n limit that the whistler instability driven by trapped electrons³⁸ can modify the parallel electron thermal conduction flux in a magnetized plasma, and magnetic field strength modulation on sheath scale can also modify the parallel thermal flux³⁹. As previously discussed after Eq. (15), the collisional electron temperature isotropization has an equally important role that is further aided by the decreasing local electric field (in magnitude) as K_n increases. An accurate E^{se} was previously found by Kaganovich²³ to be important for matching the sheath solution to the quasineutral plasma in a two-scale analysis, here we find that it enters explicitly in the Bohm speed as well. Table I also reveals that despite the mass ratio in a hydrogen plasma, ion heat flux and ion temperature isotropization can have a small but appreciable contribution to the Bohm speed. Finally, the thermal force coefficient α^{se} is directly measured from simulation data, and one can verify that Bohm speed has a very weak dependence on α^{se} for α less than or equal to the Braginskii value. For (b), we have the remarkable finding that the heat flux gradient and collisional temperature isotropization terms vary substantially in the sheath transition layer, but together they produce a Bohm speed from Eq. (11,12) that agrees accurately with simulated ion flow over space in Fig. 2. The detailed data for such a comparison is given in the supplemental material for the $K_n = 200$ case.

In conclusion, we have derived an expression for the Bohm speed that is accurate over a broad range of plasma collisionality. The Bohm speed is derived from the transport equations of an anisotropic plasma, which is expected for the sheath transition problem. This expression is verified by comparison with first-principle kinetic simulations, within the bounds set by the PIC noise. Of particular interest is that the Bohm speed thus formulated applies to the sheath transition region in which the quasineutrality is weakly perturbed. This, to our knowledge,

is the first time that a predictive formula for Bohm speed has been shown to be quantitatively accurate in the intermediate plasma regime, which is away from the known limiting cases and the asymptotic limit of $\lambda_D/L \rightarrow 0$. Our analysis can be readily extended for more complicated plasmas, and the resulting Bohm speed is consistent with the *underlying plasma transport model*. This last point accentuates the importance of an accurate plasma transport model that properly accounts for the kinetic nature of plasma transport within the Knudsen layer next to the wall, not only for bulk plasma transport, but also for the Bohm sheath constraint on wall-bound ion flow and energy flux.

We thank the U.S. Department of Energy Office of Fusion Energy Sciences and Office of Advanced Scientific Computing Research for support under the Tokamak Disruption Simulation (TDS) Scientific Discovery through Advanced Computing (SciDAC) project at both Virginia Tech under grant number DE-SC0018276 and Los Alamos National Laboratory (LANL) under contract No. 89233218CNA000001. Yanzen Zhang was supported under a Director's Postdoctoral Fellowship at LANL. This research used resources of the National Energy Research Scientific Computing Center (NERSC), a U.S. Department of Energy Office of Science User Facility operated under Contract No. DE-AC02-05CH11231. Useful discussions with Jun Li are acknowledged.

- ¹I. Langmuir, "The interaction of electron and positive ion space charges in cathode sheaths," *Phys. Rev.* **33**, 954–989 (1929).
- ²L. Tonks and I. Langmuir, "A general theory of the plasma of an arc," *Phys. Rev.* **34**, 876–922 (1929).
- ³M. A. Lieberman and A. J. Lichtenberg, *Principles of Plasma Discharges and Materials Processing*, 2nd ed. (Wiley-Interscience, 2005).
- ⁴P. C. Stangeby, *The Plasma Boundary of Magnetic Fusion Devices* (Taylor & Francis, 2000).
- ⁵A. Loarte, B. Lipschultz, A. Kukushkin, G. Matthews, P. Stangeby, N. Asakura, G. Counsell, G. Federici, A. Kallenbach, K. Krieger, A. Mahdavi, V. Philipps, D. Reiter, J. Roth, J. Strachan, D. Whyte, R. Doerner, T. Eich, W. Fundamenski, A. Herrmann, M. Fenstermacher, P. Ghendrih, M. Groth, A. Kirschner, S. Konoshima, B. LaBombard, P. Lang, A. Leonard, P. Monier-Garbet, R. Neu, H. Pacher, B. Pegourie, R. Pitts, S. Takamura, J. Terry, E. Tsitroni, the ITPA Scrape-off Layer, and D. P. T. Group, "Chapter 4: Power and particle control," *Nuclear Fusion* **47**, S203 (2007).
- ⁶D. E. Hastings and H. B. Garrett, *Spacecraft-Environment Interactions* (Cambridge University Press, Cambridge, UK, 1996).
- ⁷S. T. Lai, *Fundamentals of Spacecraft Charging: Spacecraft Interactions with Space Plasmas* (Princeton University Press, Princeton, NJ, 2011).
- ⁸D. BOHM, "The characteristics of electrical discharges in magnetic fields," *Qualitative Description of the Arc Plasma in a Magnetic Field* (1949).
- ⁹E. R. Harrison and W. B. Thompson, "The low pressure plane symmetric discharge," *Proceedings of the Physical Society* **74**, 145 (1959).
- ¹⁰K.-U. Riemann, "The bohm criterion and sheath formation," *Journal of Physics D: Applied Physics* **24**, 493–518 (1991).
- ¹¹K.-U. Riemann, "The bohm criterion and boundary conditions for a multicomponent system," *IEEE Transactions on Plasma Science* **23**, 709–716 (1995).
- ¹²S. D. Baalrud and C. C. Hegna, "Kinetic theory of the presheath and the bohm criterion," *Plasma Sources Science and Technology* **20**, 025013 (2011).
- ¹³R. M. Crespo and R. N. Franklin, "Examining the range of validity of the bohm criterion," *J. Plasma Physics* **80**, 495 (2014).
- ¹⁴S. D. Baalrud, B. Scheiner, B. Yee, M. Hopkins, and E. Barnat, "Extensions and applications of the bohm criterion," *Plasma Physics and Controlled Fusion* **57**, 044003 (2015).
- ¹⁵V. A. Godyak, R. B. Piejak, and B. M. Alexandrovich, "Probe diagnostics of non-maxwellian plasmas," *Journal of Applied Physics* **73**, 3657–3663 (1993), <https://doi.org/10.1063/1.352924>.
- ¹⁶J. E. Allen, "A note on the generalized sheath criterion," *Journal of Physics D: Applied Physics* **9**, 2331–2332 (1976).
- ¹⁷R. C. Bissell and P. C. Johnson, "The solution of the plasma equation in plane parallel geometry with a maxwellian source," *The Physics of Fluids* **30**, 779–786 (1987).
- ¹⁸K.-U. Riemann, "Plasma-sheath transition in the kinetic tonks-langmuir model," *Physics of Plasmas* **13**, 063508 (2006), <https://doi.org/10.1063/1.2209928>.
- ¹⁹K.-U. Riemann, "Comment on 'kinetic theory of the presheath and the bohm criterion'," *Plasma Sources Science and Technology* **21**, 068001 (2012).
- ²⁰S. D. Baalrud and C. C. Hegna, "Reply to comment on 'kinetic theory of the presheath and the bohm criterion'," *Plasma Sources Science and Technology* **21**, 068002 (2012).
- ²¹V. A. Godyak and N. Sternberg, "Smooth plasma-sheath transition in a hydrodynamic model," *IEEE Transactions on Plasma Science* **18**, 159–168 (1990).
- ²²R. N. Franklin, "You cannot patch active plasma and collisionless sheath," *IEEE Transactions on Plasma Science* **30**, 352–356 (2002).
- ²³I. D. Kaganovich, "How to patch active plasma and collisionless sheath: A practical guide," *Physics of Plasmas* **9**, 4788–4793 (2002), <https://doi.org/10.1063/1.1515274>.
- ²⁴V. Godyak and N. Sternberg, "Good news: you can patch active plasma and collisionless sheath," *IEEE Transactions on Plasma Science* **31**, 303–303 (2003).
- ²⁵K.-U. Riemann, "Kinetic analysis of the collisional plasma-sheath transition," *Journal of Physics D: Applied Physics* **36**, 2811–2820 (2003).
- ²⁶R. N. Franklin, "Where is the sheath edge?" *Journal of Physics D: Applied Physics* **37**, 1342–1345 (2004).
- ²⁷R. N. Franklin and J. R. Ockendon, "Asymptotic matching of plasma and sheath in an active low pressure discharge," *Journal of Plasma Physics* **4**, 371–385 (1970).
- ²⁸N. Sternberg and V. Godyak, "On asymptotic matching and the sheath edge," *IEEE Transactions on Plasma Science* **31**, 665–677 (2003).
- ²⁹X. Z. Tang, "Kinetic magnetic dynamo in a sheath-limited high-temperature and low-density plasma," *Plasma Physics and Controlled Fusion* **53**, 082002 (2011).
- ³⁰R. Chodura and F. Pohl, "Hydrodynamic equations for anisotropic plasmas in magnetic fields. II. transport equations including collisions," *Plasma Physics* **13**, 645–658 (1971).
- ³¹X.-Z. Tang and Z. Guo, "Critical role of electron heat flux on bohm criterion," *Physics of Plasmas* **23**, 120701 (2016), <https://doi.org/10.1063/1.4971808>.
- ³²X.-Z. Tang and Z. Guo, "Kinetic model for the collisionless sheath of a collisional plasma," *Physics of Plasmas* **23**, 083503 (2016), <https://doi.org/10.1063/1.4960321>.
- ³³B. K. J. Bowers, B. J. Albright and T. Kwan, "Ultrahigh performance three-dimensional electromagnetic relativistic kinetic plasma simulation," *Phys. Plasmas* **10**:1, 183 (2008).
- ³⁴See the supplemental material for the plasma profile and a comparison of simulation data with the collisional closure of Chodura and Pohl, which includes Refs.[29,30,35].
- ³⁵T. Takizuka and H. Abe, "A binary collision model for plasma simulation with a particle code," *Journal of Computational Physics* **25**, 205 – 219 (1977).
- ³⁶The nominal sheath Knudsen number is computed with initial plasma parameters for an isotropic plasma before the sheath is dynamically formed with absorbing walls and an upstream source. The local sheath Knudsen number is computed with local plasma parameters after the steady-state sheath is established, so it varies with position.
- ³⁷Chodura and Pohl's collisional closure captures the trend but is less accurate than closure flux from kinetic simulations in predicting the Bohm speed, as expected.
- ³⁸Z. Guo and X.-Z. Tang, "Ambipolar transport via trapped-electron whistler instability along open magnetic field lines," *Phys. Rev. Lett.* **109**, 135005 (2012).
- ³⁹Z. Guo and X.-Z. Tang, "Parallel heat flux from low to high parallel temperature along a magnetic field line," *Phys. Rev. Lett.* **108**, 165005 (2012).

Supplemental material to “Bohm criterion of plasma sheaths away from asymptotic limits”

(Dated: January 28, 2022)

arXiv:2201.1191v1 [physics.plasm-ph] 26 Jan 2022

Here we provide supplemental information on the simulation setup, presheath and sheath plasma profile, and the transport flux and Bohm speed evaluated from first-principles particle-in-cell simulations. Specifically the detailed profile for a slab plasma with a collisional presheath from the kinetic simulation, shows a smooth transition region between the presheath and the sheath, and demonstrates the anisotropic nature of the plasma due to the decompressional cooling, section I. The temperature isotropization terms Q_{ee} and Q_{ei} are calculated directly from the kinetic simulation and compared with Chodura’s closure, demonstrating the needs for kinetic corrections to closure flux where local Knudsen number is large, section II. Finally in section III we document the data comparison between the predicted Bohm speed and the observed ion out flow speed over a sheath transition region, and how different physical mechanisms come together to set the Bohm speed.

I. SIMULATION SETUP AND STEADY-STATE PLASMA PROFILE

Our simulations consider a slab plasma bounded by two absorbing walls, with an upstream source in the middle that compensates the particle and energy loss to the walls. The plasma parameters are averaged over 10000 time steps after reaching the steady state in order to reduce the noise from the PIC simulation. The steady-state plasma profile for a plasma with collisional presheath ($K_n \equiv \lambda_{mfp}/\lambda_D = 75$) are shown in Fig. 1. The density and temperature of both species are normalized to their initial values n_0 and T_0 , the potential ϕ to T_0/e , the ion flow to the local adiabatic sound speed $c_s = \sqrt{(T_e + 3T_i)/m_i}$.

The electron temperature is anisotropic within the Knudsen layer (from the wall to λ_{mfp} , which is about $19.9\lambda_D$) due to decompressional cooling in the x -direction for a collisionless case[1]. Further upstream, the strong Coulomb collisions eliminate the electron temperature anisotropy. Strong ion temperature anisotropy extends much further upstream due to the slow ion-electron and ion-ion collision rate. In steady state, the plasma temperature gradient exists in the presheath and sheath region. The nominal sheath entrance is beyond $x = 5\lambda_D$, where the fractional charge gradient is 10% and the ion exit flow is supersonic. These observations indicate that more involved transport physics need to be considered in the presheath-sheath transition problem.

II. COMPARISON OF TEMPERATURE ISOTROPIZATION TERMS FROM KINETIC SIMULATION TO CHODURA’S CLOSURE

The presheath/sheath plasma within a mean-free-path from the wall has anisotropic temperature due to decompressional cooling in the flow direction. Coulomb collisions among

plasma particles can affect their momentum and energy transport. The momentum transfer due to Coulomb collisions between electrons and ions consists of two components, the frictional force due to the net current j and the thermal force caused by the temperature gradient. Here we consider the cases with no net current so frictional force can be neglected. In an anisotropic plasma, the collisional energy exchange consists of temperature equilibration between different species, relaxation of temperature anisotropy, and Ohmic heating. In the presheath to sheath transition problem, Ohmic heating is negligible in the absence of net current j and the temperature equilibration between different species is negligible due to the large ion-electron mass ratio. The dominant term in energy exchange is temperature isotropization. For the reason we explained in the paper, despite not being a gradient term in the plasma transport equation, it can play a critically important role in Bohm criterion analysis, along with the more obvious leading order terms in the multi-scale expansion of heat flux q_n and thermal force R_T , which are gradient terms.

To verify that our newly derived Bohm speed agrees with direct measurement of ion exit flow speed in the sheath transition region, we compute heat flux, thermal force, and collisional isotropization terms directly from kinetic simulation data. Specifically, the momentum energy transfer rate of species a due to collisions with species b can be evaluated from the summation over the particle population,

$$\begin{aligned} I_\alpha^{ab} &= \int m_a v_\alpha \left(\frac{\partial f}{\partial t} \right)_{coll}^{ab} d^3 v \\ &= \frac{N_f}{\Delta t} m_a \int \sum_{i=1}^{N_a} (\delta^3(v - v'_i) - \delta^3(v - v_i)) v_\alpha d^3 v \quad (1a) \\ &= \frac{N_f}{\Delta t} m_a \sum_{i=1}^{N_a} \Delta v_{i\alpha}^{ab} \end{aligned}$$

$$\begin{aligned} J_{\alpha\beta}^{ab} &= \int m_a (v_\alpha - V_\alpha)(v_\beta - V_\beta) \left(\frac{\partial f}{\partial t} \right)_{coll}^{ab} d^3 v \\ &= \int m_a v_\alpha v_\beta \left(\frac{\partial f}{\partial t} \right)_{coll}^{ab} d^3 v - V_\alpha I_\alpha^{ab} - V_\beta I_\beta^{ab} + V_\alpha V_\beta S^{ab} \\ &= \frac{N_f}{\Delta t} m_a \sum_{i=1}^{N_a} (v'_{i\alpha} v'_{i\beta} - v_{i\alpha} v_{i\beta}) - V_\alpha I_\alpha^{ab} - V_\beta I_\beta^{ab} \quad (1b) \end{aligned}$$

where α and β are directions, N_f is a normalizing factor and N_a is the total number of super particles of species a in the simulation. S^{ab} is the density change rate and it equals 0 for Coulomb collisions. Here $(\partial f/\partial t)_{coll}^{ab}$ is the change of the distribution function due to the Coulomb collision between species a and b and it is evaluated using Takizuka and Abe’s method [2] in VPIC. It can be noted that Takizuka and Abe’s method ensures momentum and energy conservation in binary collisions, to the machine accuracy in floating point calculations on a computer. In the case of no net current and slow

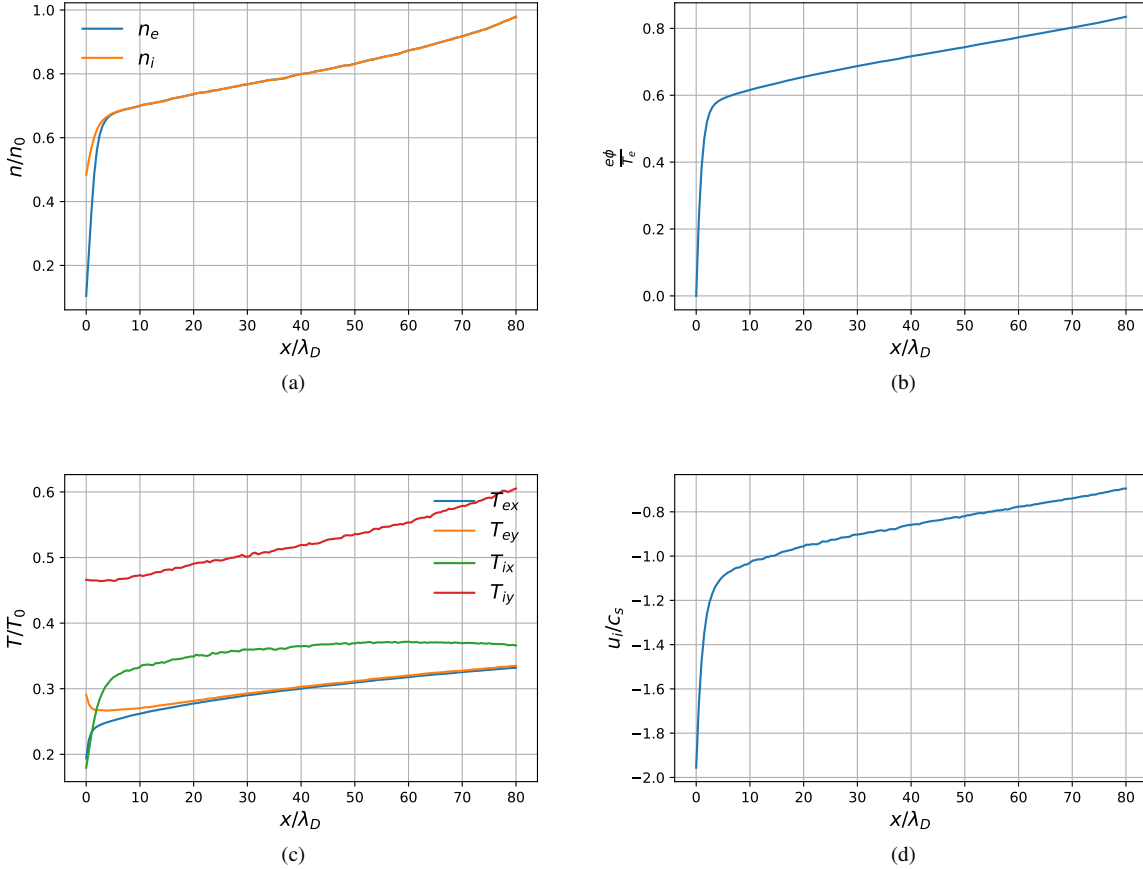


FIG. 1: Steady-state presheath and sheath profile: (a) densities of electrons and ions normalized by the initial density n_0 ; (b) plasma potential normalized by T_e/e ; (c) temperatures of electron and ion in x (normal to the wall) and y (tangential to the wall) direction, normalized by the initial temperature T_0 ; (d) ion flow velocity normalized by the adiabatic sound speed $c_s = \sqrt{(T_{ex} + 3T_{ix})/m_i}$;

temperature relaxation rate between different species, thermal force R_T and the temperature isotropization Q can be directly obtained from Eq. 1a and Eq. 1b in a PIC simulation.

In the collisional limit, Chodura and Pohl provide a closure for the anisotropic plasma transport [3]. In present analysis, we focus on cases where the collisional mean-free-path is much longer than the Debye length. Furthermore, the plasma distribution functions are skewed by the free-streaming loss so kinetic corrections to Chodura's closure are expected. Here, we contrast the temperature isotropization terms $Q_{ee,ei}$ obtained by Eq. 1b with those calculated from Chodura's expression (see Eq. 6 in the paper) in Fig. 2

From Fig. 2, one can see that while Chodura's closure captures the underlying collisional isotropization physics admirably, kinetic correction in Q_{ei} is important for accurate evaluation of Bohm speed using Eq. (12) of the paper.

III. BOHM SPEED VARIATION IN THE SHEATH TRANSITION REGION

To show the validity of the Bohm speed model over a sheath transition region rather than one single point at the sheath entrance, aside from Fig. (2) in the paper, here we provide the value of the physical quantities for evaluating the Bohm speed in Eq. (12) of the paper over a small region $x \in [5.0\lambda_D, 10.0\lambda_D]$ near the sheath entrance in Table.I.

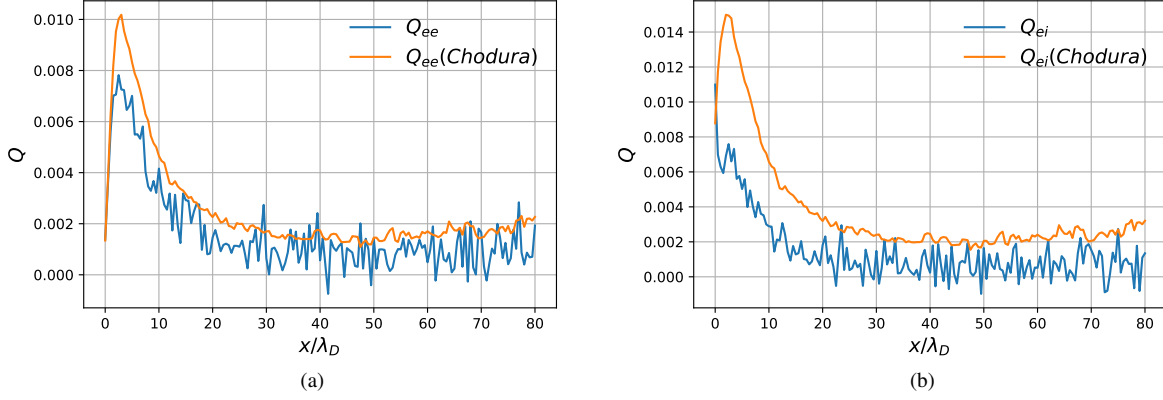


FIG. 2: Comparison of Q_{ee} and Q_{ei} terms evaluated from kinetic simulation with those calculated by Chodura's closure for a collisional presheath with $K_n = 75$.

TABLE I: Normalized parameters determining the Bohm speed in the sheath transition region for $K_n = 200$.

x	u_{ix}^{se}	u_{Bohm}	$\frac{1}{e\Gamma_e^{se}} \frac{\partial q_n^e}{\partial \phi}$	$\frac{Q_{ee}^{se} + Q_{ei}^{se}}{e\Gamma_e^{se} E^{se}}$	$\frac{1}{e\Gamma_e^{se}} \frac{\partial q_n^i}{\partial \phi}$	$\frac{Q_{ii}^{se}}{e\Gamma_e^{se} E^{se}}$	α
$\frac{x}{\lambda_D}$	c_s	c_s					
5.0	1.04	1.01	-1.67	3.05	-0.21	0.33	0.39
5.5	1.03	1.00	-2.20	3.55	-0.22	0.38	0.45
6.0	1.02	0.99	-2.77	4.02	-0.24	0.46	0.49
6.5	1.01	1.00	-3.15	4.11	-0.24	0.48	0.44
7.0	1.00	0.99	-3.23	4.33	-0.27	0.55	0.47
7.5	0.99	1.00	-3.46	4.57	-0.30	0.54	0.49
8.0	0.99	0.99	-3.92	4.72	-0.20	0.54	0.41
8.5	0.98	0.97	-4.19	5.03	-0.17	0.63	0.44
9.0	0.98	0.96	-4.38	5.35	-0.20	0.66	0.51
9.5	0.97	0.97	-4.45	5.40	-0.22	0.63	0.49
10.0	0.97	0.97	-4.11	4.93	-0.25	0.70	0.50

The model gives an accurate prediction for the Bohm speed over the sheath transition region as is shown by comparing the second and third column in Table.I. Even though the normalized physical quantities, such as heat flux and temperature isotropization rate, vary enormously in the sheath transition region, those large changes compensate with each other to capture the slowly varying ion exit flow speed or Bohm speed in the sheath transition region.

[1] X. Z. Tang, Plasma Physics and Controlled Fusion **53**, 082002 (2011).
 [2] T. Takizuka and H. Abe, Journal of Computational Physics **25**,

205 (1977).
 [3] R. Chodura and F. Pohl, Plasma Physics **13**, 645 (1971).